Rapid analysis of the microfibril angle of loblolly pine from two test sites using near-infrared analysis

by Chi-Leung So[1,*], Jennifer H. Myszewski[2], Thomas Elder[3] and Leslie H. Groom[3]

ABSTRACT

There have been several recent studies employing near infrared (NIR) spectroscopy for the rapid determination of microfibril angle (MFA). However, only a few have utilized samples cut from individual rings of increment cores, and none have been as large as this present study, sampling over 600 trees from two test sites producing over 3000 individual ring samples for MFA analysis. This has allowed the use of individual growth ring models rather than using those based on earlywood, latewood, corewood or outerwood. It was observed that for both test sites, the strongest models were from the "All", earlywood and latewood sample sets. The individual growth ring calibration models provided poorer RPD values despite using over 200 samples in the analyses. In general, the results from the test samples largely mirrored those from the corresponding calibration samples. Corresponding test sample predictions from the opposing site were noticeably poorer than test samples from the same site. Thus, a greater variation in the number of sites would provide improved model robustness. This study has found that the models based on individual ring samples were not as strong as those obtained in other studies based on the radial-longitudinal face of wood strips, spread over several growth rings.

Keywords: near infrared spectroscopy, multivariate analysis, microfibril angle, loblolly pine, *Pinus taeda* L.

RÉSUMÉ

Il y a eu de nombreuses études récentes employant la spectroscopie proche infrarouge (PIR) pour la détermination rapide de l'angle des microfibrilles (AMF). Cependant, seules quelques-unes ont utilisé des échantillons extraits de cernes individuels sur des carottes de bois, et aucune n'a été aussi étendue que cette présente étude avec plus de 600 arbres échantillonnés sur deux sites d'essai produisant plus de 3000 échantillons de cernes individuels pour les analyses d'AMF. Cela a permis d'utiliser des modèles de cernes de croissance individuels plutôt que d'utiliser ceux basés sur le bois de printemps, le bois d'été, le bois interne ou externe. Il a été observé que pour les deux sites d'essai, les modèles les plus robustes étaient obtenus à partir de l'ensemble des échantillons (« All »), bois de printemps et bois d'été. Les modèles d'étalonnage pour les cernes de croissance individuels ont fourni des valeurs de RPD plus faibles malgré l'utilisation de plus de 200 échantillons dans l'analyse. En général, les résultats des échantillons d'essais ont largement reflété ceux des échantillons d'étalonnage correspondants. Les échantillons d'essais prédits à partir du site opposé étaient notablement plus faibles que les échantillons d'essais correspondants prédits à partir du même site. Par conséquent, une plus grande variation dans le nombre de sites permettrait d'obtenir des modèles plus robustes. Cette étude a montré que des modèles basés sur des échantillons de cernes individuels n'étaient pas aussi robustes que ceux obtenus dans d'autres études basées sur la section radiale-longitudinale de bandes de bois, étendue sur plusieurs cernes de croissance.

Mots clés : spectroscopie proche infrarouge, analyses multi-variées, angle des microfibrilles, pin à torches, *Pinus taeda* L.

Introduction

Timber harvesting for both industrial and private landowners is primarily volume-based; however, wood quality characteristics have generally had neutral or slightly unfavorable genetic correlations with volume growth (Byram *et al.* 2005). One of the important traits of interest is microfibril angle (MFA), defined as the angle between the cell axis and the cellulose microfibrils of the S-2 layer of the cell wall of which it is composed. MFA plays an important role in both the mechanical properties and the dimensional stability of wood that, together with density, can account for almost all of the stiffness of wood (Cave and Walker 1994, Megraw *et al.* 1998). Donaldson (2008) has published an extensive literature review of microfibril angle, with particular emphasis on its measurement, variation and relationships.

Despite its obvious importance to wood quality, MFA is not commonly assessed in tree improvement programs, mainly due to the time and/or expense of measuring MFA on a large scale with the current methods available (Schimleck and Evans 2002, Myszewski *et al.* 2004). Conventional techniques for determining MFA include x-ray diffraction (XRD) (Cave and Walker 1994, Megraw *et al.* 1998), polarized microscopy (El-Hosseiny and Page 1973) and pit aperture measurements (Donaldson 1991). Based on XRD, SilviScan has been very successfully employed for rapid MFA measurements along increment cores (Evans 1997, 1999; Evans and Illic 2001). This instrument utilizes a combination of x-ray diffractometry, x-ray densitometry and image analysis for the rapid determination of a range of wood properties at high spatial resolution.

[1]School of Renewable Natural Resources, Louisiana State University AgCenter, Baton Rouge, LA.
[2]formerly of Southern Institute of Forest Genetics, USDA Forest Service, Saucier, MS.
[3]Utilization of Southern Forest Resources, USDA Forest Service, Pineville, LA.
[*]Corresponding author: E-mail: cso@agcenter.lsu.edu

The use of near infrared (NIR) spectroscopy for the characterization of wood has gained considerable interest throughout the forest products industry (So *et al*. 2004). This technique is rapid, relatively low-cost, non-destructive, and requires minimal sample preparation. NIR spectroscopy, coupled with multivariate analysis, is gaining wide use for the prediction of a variety of wood properties (Hoffmeyer and Pedersen 1995, Gindl *et al*. 2001, Kelley *et al*. 2004). Similarly, NIR spectroscopy has used SilviScan data to obtain excellent calibrations for a variety of wood properties such as density and stiffness (Jones *et al*. 2005, Schimleck *et al*. 2005).

There have been several studies using NIR spectroscopy to determine MFA. NIR models of MFA based on SilviScan data have yielded excellent calibrations (Schimleck and Evans 2002, Jones *et al*. 2005, Schimleck *et al*. 2005). In these studies, spectra were collected from the radial-longitudinal face of wooden strips cut from increment cores, and averaged over 10 mm increments, and as a consequence, it was not possible to follow the variation of MFA on an annual basis to observe the effects of silvicultural treatments. Inter-ring variability has been assessed by sectioning individual early wood and late wood rings from increment cores and collecting NIR spectra from the tangential face (Kelley *et al*. 2004, Schimleck *et al*. 2007, Via *et al*. 2007, Hein *et al*. 2010). Kelley *et al*. (2004) obtained reasonable correlations with MFA from loblolly pine (*Pinus taeda* L.); however, only 72 total samples were used in the analysis. Furthermore, the MFA calibrations were reported poorer than those obtained for a range of chemical and mechanical properties in the same study. This was attributed to the relatively large experimental errors associated with measuring MFA using x-ray diffraction. A larger NIR study, with 451 samples, was undertaken by Schimleck *et al*. (2007) in which strong MFA correlations were obtained from early wood and late wood sample sets, as well as the complete set. The predictive ability of the calibrations was similarly strong. With approximately 4500 MFA samples taken from 632 trees of this large-scale genetic program, the purpose of this NIR study was to compare MFA calibrations between earlywood and latewood, corewood and outerwood, as well as the complete set, and to assess their ability to predict MFA for individual growth ring samples.

Materials and Methods

Sampling

Twelve-millimeter increment cores were collected at breast height (1.37 m) from loblolly pine trees from two progeny test sites in Ashley County, AR. GP065 and GP258 were established in 1974 and 1978, respectively, by Georgia Pacific Corporation. At the time of sampling, GP065 and GP258 were 20 and 25 years old, respectively. In total, cores were extracted from 335 trees in GP065 and 297 trees in GP258. Complete descriptions of the test sites and genetic sampling methods are available in Myszewski *et al*. (2004).

Specimen preparation

Growth rings 4 and 5 were selected to represent core wood while outer wood was represented by rings 19 and 20. Individual earlywood (EW) and latewood (LW) rings were carefully cut and sectioned from the increment cores using a razor blade, as described in Megraw *et al*. (1998). Each circular EW or LW wafer specimen was optically evaluated for any contamination from adjacent EW or LW material, and assigned to appropriate sample sets, such as corewood (core), outerwood (outer), earlywood (EW) or latewood (LW), and growth ring number. For example, the latewood growth ring sample from ring 20 was assigned LW20. Earlywood 20 (EW20) and latewood 19 (LW19) samples from the GP065 test site were excluded due to very narrow growth rings leading to the possibility of contamination from adjacent EW or LW material. Further details of specimen preparation are described in Myszewski *et al*. (2004).

Microfibril angle measurement

Over 3000 individual MFA measurements were collected by Dr. Robert Megraw (Weyerhaeuser, retired), at the Department of Forest Science, Texas A&M, College Station, TX, using a GE XRD-7 diffractometer. A copper target was used at an accelerating voltage of 50 kV. MFA reproducibility was determined to be ±1° with 95% confidence, achieved by running the same sample several times. The MFA technique used is fully described in Megraw *et al*. (1998).

NIR spectroscopy

NIR spectra of the individual MFA samples were collected, between 1000 nm and 2500 nm, using a Nexus 670 FTIR spectrometer, equipped with a NIR Fiberport accessory (both Thermo Nicolet Instruments, Madison, WI). The wood samples of known MFA were placed directly on to the window of the accessory providing a spot size of 6 mm diameter. Two spectra were collected for each sample (one from each face).

Multivariate analysis

Multivariate analysis of the data was performed using the Unscrambler (vsn. 8.0) software, CAMO (Woodbridge, NJ). The NIR data were first averaged to one spectrum per sample. Partial least squares (PLS) regression was used to predict MFA values for the samples. Multiplicative scatter correction (MSC) was applied to the NIR data prior to modeling. Each sample set was randomly separated into calibration and test sets with three-quarters used for calibration and the remainder for testing. Models were generated using full cross validation (Martens and Naes 1989) and were assessed using several common measures of calibration performance, such as the coefficient of determination, R^2, which is a measure of the strength of the fit to the data. The standard errors of calibration (SEC), cross validation (SECV) and prediction (SEP) were determined from the residuals of the calibrations, each cross validation phase and predictions, respectively. A high SECV indicates that the sample excluded in each cross validation phase was not well predicted by the corresponding calibration. SEP provides a measure of the effectiveness of a calibration in predicting the parameter of interest for an unknown set of samples. The ratio of performance to deviation (RPD) is a parameter that accounts for the variability in the data and is calculated as the ratio of the standard deviation of the reference data to the SECV or SEP (Williams and Sobering 1993).

Results and Discussion

Microfibril angle

MFA measurements were collected using XRD (Myszewski *et al*. 2004) and the results are shown in Tables 1a and 1b for GP258 and GP065 test sites, respectively. These include: the range and mean of MFA values for each sample set, as well as the standard deviation and coefficient of variation (CV). The

Table 1a. MFA statistics for GP258 test site

	Calibration					Test				
Sample set	N	MFA range (°)	Mean MFA (°)	SD (°)	CV (%)	N	MFA range (°)	Mean MFA (°)	SD (°)	CV (%)
All	1897	5-54	31.6	10.8	34.3	629	6-53	31.5	10.8	34.2
Core	954	23-54	40.1	4.3	10.8	316	20-52	39.9	4.7	11.8
Outer	943	5-40	22.9	8.4	36.7	313	6-46	23.2	8.2	35.4
EW	951	5-54	32.3	9.1	28.3	315	6-52	32.2	9.3	28.8
LW	946	6-53	30.9	12.3	39.7	314	6-50	30.7	12.0	39.1
EW4	237	27-54	39.0	4.3	11.1	79	30-47	39.5	4.2	10.5
LW4	239	28-50	41.4	4.3	10.3	79	20-50	40.9	4.9	11.9
EW5	240	23-48	38.8	3.9	10.0	79	26-52	39.1	4.4	11.2
LW5	238	27-53	41.1	4.2	10.3	79	22-48	40.0	5.0	12.5
EW19	237	5-40	25.1	7.7	30.8	79	6-46	26.2	7.4	28.2
LW19	235	6-39	21.1	8.2	38.7	78	7-37	20.8	7.9	37.9
EW20	237	5-39	25.7	8.0	30.9	78	6-41	25.2	7.5	29.5
LW20	234	6-38	20.0	8.3	41.5	78	6-36	20.0	8.6	43.2

Table 1b. MFA statistics for GP065 test site

	Calibration					Test				
Sample set	N	MFA range (°)	Mean MFA (°)	SD (°)	CV (%)	N	MFA range (°)	Mean MFA (°)	SD (°)	CV (%)
All	1485	7–54	36.6	9.6	26.3	492	8–52	35.9	9.9	27.5
Core	994	21–54	41.9	4.1	9.8	330	25–52	41.5	4.2	10.1
Outer	491	7–43	25.9	8.7	33.6	162	8–45	24.8	8.5	34.3
EW	742	10–50	37.7	6.9	18.2	246	20–50	37.7	6.9	18.3
LW	743	7–54	35.6	11.7	32.8	246	8–52	34.1	12.0	35.0
EW4	246	29–50	41.4	3.4	8.2	82	32–50	41.1	3.7	9.1
LW4	249	21–54	43.1	4.3	9.9	83	32–52	42.8	4.1	9.5
EW5	251	25–50	41.1	3.8	9.1	83	33–49	41.3	4.0	9.7
LW5	248	25–53	41.8	4.6	11.0	82	25–52	40.9	4.9	12.0
EW19	245	10–43	30.4	6.1	20.0	81	20–45	30.0	5.4	18.0
LW19	–	–	–	–	–	–	–	–	–	–
EW20	–	–	–	–	–	–	–	–	–	–
LW20	246	7–40	21.3	8.4	40.0	81	8–36	20.0	8.2	40.8

mean MFA values for these sample sets have been previously discussed by Myszewski *et al.* (2004); however, the values used in this study are slightly different due to the creation of calibration and test sets for model-building within each of the sample sets as shown in Tables 1a and 1b. Earlywood 20 (EW20) and latewood 19 (LW19) samples from the GP065 test site were not analyzed due to their narrow growth rings leading to possible contamination from adjacent EW or LW rings (Myszewski *et al.* 2004). This resulted in a disproportionately smaller amount of low MFA samples. Thus, the mean MFA values for the larger combined GP065 sample sets in Table 1b were noticeably higher than their GP258 counterparts in both the calibration and test sets (Table 1a). For example, the "All", "EW" and "LW" GP065 calibration samples had mean MFA values approximately 5° greater than their GP258 counterparts.

The clearest differences for both test sites were, as expected, between the mean MFA values of the corewood and outerwood (Tables 1a and 1b). The corewood GP258 calibration samples had a much higher mean MFA (40.1°) compared with the corresponding outerwood (22.9°). The MFA range was also much smaller for these samples (23°–54°) than their corresponding outerwood samples (5°–40°), contributing to the much lower standard deviations and CVs. This was particularly evident for the CVs, which were 10.8% and 36.7% for the corewood and outerwood, respectively. The outerwood (EW19 to LW20) exhibited much wider MFA ranges than their corewood (EW4 to LW5) counterparts, contributing to their higher standard deviations. Myszewski *et al.* (2004) noted the wide range of MFA values in these samples was probably due to the very large sample size and the presence of compression wood in the cores. It is possible that the samples with high MFA values (greater than 40°) for the outerwood were compression wood, although, these samples were not excluded from the analysis (Myszewski *et al.* 2004). The outerwood and corewood variation was

similarly reflected in their values of standard deviation and CV. Shupe *et al*. (1996) obtained low standard deviations (3°–5°) from latewood tracheids of corewood and outerwood in a study of nine-year-old loblolly pine, in which rings 7 to 9 were designated as the outerwood. The CVs ranged from 10% to 12%, similar to that observed for the corewood sample sets in our present study. A larger increase in CV (13.0%–21.7%) was obtained from rings 5 to 20 of latewood fibres from the earlier study by Mott *et al*. (2002) with the CV reaching 34.1% for growth ring 40 (Groom *et al*. 2002). Via *et al*. (2007) reported a greater range of CVs (15%–55%) in a MFA study of 41-year-old longleaf pine trees, ranging from 15.7% (growth ring 4) to 55.8% (growth ring 16).

It was noted that the GP258 earlywood calibration provided a slightly higher mean MFA (32.3°) than its latewood counterpart (30.9°). Similar trends were also observed by Schimleck *et al*. (2007) in a MFA study of loblolly pine for earlywood and latewood specimens with average MFA values of 30.7° and 27.7°, respectively. The large differences in standard deviation and CV between these sets can be clearly attributed to the outerwood, with only small differences observed in the corewood. These differences in the core/outer and EW/LW sample sets can be more clearly seen using the individual samples sets. The mean MFA values for the EW outerwood (EW19 and EW20) were higher than that for their LW counterparts (LW19 and LW20); however, the converse was true for the corewood samples. This was also observed by Megraw *et al*. (1998). They also noted that the transition between the earlywood/latewood MFA varies with tree height. Closer to the base of the tree, the relationship between earlywood and latewood MFA reverses at a greater number of rings from the pith than it does further up the bole. Mott *et al*. (2002) had previously observed higher MFA values for earlywood loblolly pine fibres than with latewood fibres for growth rings 5 and 10. However, this was also observed for growth rings 20 and 40, though not rings 30 and 48. Clark *et al*. (2006) noted it was difficult to estimate the age of transition for the juvenile wood to mature wood as the transition is gradual in loblolly pine.

Multivariate analysis

Partial least squares (PLS) regression was carried out using the NIR and MFA data. With both test sites, calibration models were built for each sample set and tested using their corresponding test set. These models also underwent further testing using the corresponding test set from the other site.

Calibration models

With the large number of samples, up to 15 factors were employed in the analyses. The number was recommended by the software, based on the significance of the change in variance. The coefficient of determination (R^2), SEC, SECV and RPD values for the analyses are listed in Tables 2a and 2b for GP0258 and GP065, respectively. The calibration models were built employing between eight and 15 factors, with most of the combined, larger samples sets using nine or 10 factors. The MFA calibration plot for the "All" GP258 sample set is shown in Fig. 1. This calibration was built with 1897 samples using only 10 factors, providing an R^2 of 0.85, SEC of 4.2°, SECV of 4.3° and a RPD of 2.54. A RPD value of 2.5 and above is considered acceptable for screening purposes (Williams and Sobering 1993). The "All" GP065 provided similar results (R^2 = 0.85; SECV = 3.8°; RPD = 2.51) using nine factors. These values are in fairly good agreement (R^2 = 0.87; SEC = 4.28°; SECV = 5.55°; RPD = 2.31; 10 factors) with a NIR study of the tangential face of loblolly pine samples utilizing 317 calibration samples (Schimleck *et al*. 2007). Kelley *et al*. (2004) also used similar specimens of loblolly pine, but with a much smaller number of calibration samples (44), in which a calibration value of R^2 = 0.68 (R = 0.82) and an RMSEC of 5.7° were obtained using a broader wavelength range (500–2400 nm) and five factors. At low MFA, especially below 15°, the calibration data plotted in Fig. 1 appear to show a slight deviation (predicting higher MFA) from the 1:1 equivalence line. This can also be seen in the residuals plot (Fig. 2), in which each residual is the difference between the NIR and XRD-determined MFA values. There were twice as many residuals

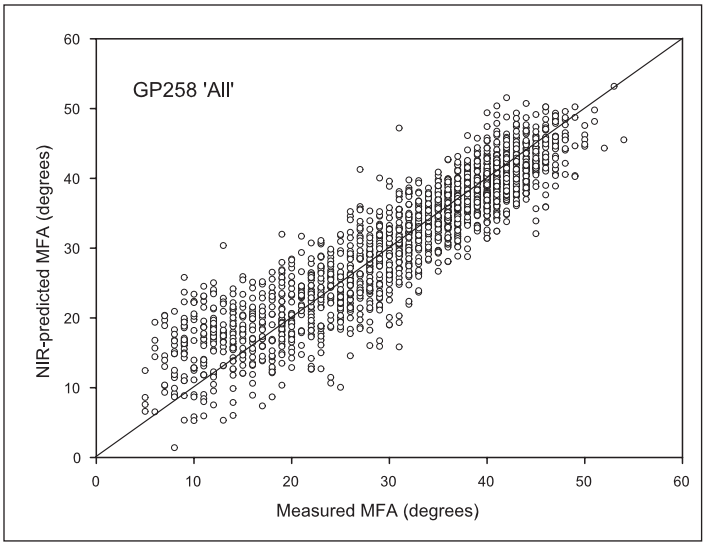

Fig. 1. Relationship between the NIR- and XRD-determined MFA for the "All" calibration samples from GP258.

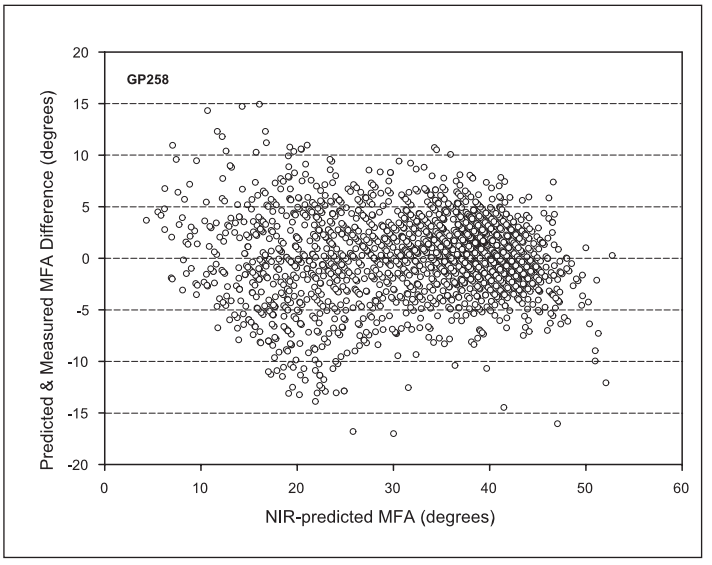

Fig. 2. Residuals for the MFA results in Fig. 1.

Table 2a. PLS statistics for GP258 test site

Sample set	Factors	GP258 Calibration R^2	SEC (°)	SECV (°)	RPD	GP258 Test R^2	SEP (°)	RPD	GP065 Test R^2	SEP (°)	RPD
All	10	0.85	4.2	4.3	2.54	0.84	4.4	2.47	0.78	4.9	2.00
Core	15	0.66	2.5	2.6	1.65	0.74	2.4	1.96	0.62	2.6	1.62
Outer	10	0.72	4.5	4.6	1.84	0.67	4.7	1.74	0.54	6.1	1.41
EW	9	0.85	3.5	3.6	2.53	0.84	3.7	2.52	0.78	3.5	1.99
LW	9	0.85	4.7	4.8	2.55	0.85	4.7	2.57	0.79	5.7	2.09
EW4	13	0.67	2.5	2.9	1.50	0.60	2.7	1.54	0.34	3.3	1.14
LW4	11	0.61	2.7	2.9	1.46	0.73	2.6	1.91	0.58	2.7	1.52
EW5	13	0.66	2.3	2.6	1.50	0.64	2.7	1.65	0.40	3.1	1.29
LW5	12	0.66	2.5	2.7	1.55	0.71	2.7	1.87	0.77	2.4	2.05
EW19	10	0.76	3.8	4.2	1.83	0.68	4.3	1.73	0.49	4.2	1.28
LW19	11	0.70	4.5	5.0	1.63	0.71	4.3	1.84	–	–	
EW20	8	0.82	3.4	3.6	2.21	0.73	4.0	1.85	–	–	
LW20	10	0.70	4.6	5.1	1.65	0.65	5.1	1.69	0.39	7.5	1.09

Table 2b. PLS statistics for GP065 test site

Sample set	Factors	GP065 Calibration R^2	SEC (°)	SECV (°)	RPD	GP065 Test R^2	SEP (°)	RPD	GP258 Test R^2	SEP (°)	RPD
All	9	0.85	3.8	3.8	2.51	0.84	3.9	2.51	0.73	5.7	1.89
Core	10	0.64	2.5	2.6	1.61	0.63	2.6	1.64	0.63	2.9	1.65
Outer	10	0.72	4.6	4.9	1.79	0.68	4.9	1.76	0.48	6.0	1.36
EW	10	0.82	2.9	3.0	2.28	0.80	3.1	2.21	0.78	4.3	2.14
LW	10	0.90	3.8	4.0	2.94	0.88	4.1	2.94	0.78	5.7	2.11
EW4	10	0.59	2.2	2.4	1.42	0.43	2.8	1.32	0.52	2.9	1.43
LW4	11	0.67	2.5	2.7	1.56	0.68	2.3	1.73	0.64	3.0	1.63
EW5	13	0.67	2.1	2.5	1.53	0.60	2.5	1.58	0.40	3.8	1.17
LW5	10	0.73	2.4	2.6	1.74	0.80	2.2	2.24	0.40	4.8	1.04
EW19	8	0.63	3.7	4.0	1.53	0.44	4.0	1.33	0.62	4.5	1.63
LW19	–	–	–	–	–	–	–		–	–	–
EW20	–	–	–	–	–	–	–		–	–	–
LW20	11	0.71	4.6	5.1	1.65	0.62	5.1	1.61	0.23	9.2	0.94

greater than -10° compared with +10°. However, these accounted for only a very small number of the samples. The rest of the samples (i.e., 97%) were evenly divided between positive and negative residuals with values between ±10°. Almost 75% of the samples had residuals between ±5°. Schimleck *et al*. (2007), analyzing tangential sections, had reported many large residuals, in which the magnitude of the residuals were also evenly spread across the MFA range.

Separating out the EW and LW sample sets provided similar R^2 values when compared with the "All" sample sets. The EW and LW calibrations for the GP258 samples both utilized nine factors, providing identical R^2 values of 0.85 and very similar RPD values (2.53 and 2.55, respectively), even though the EW calibration provided a lower SECV value (3.6°) than the LW (Table 2a). For the GP065 site, the EW and LW calibrations both utilized 10 factors. A higher R^2 of 0.90 was obtained for the LW calibration compared with the EW calibration, together with higher values of SECV (4.0°) and RPD (2.94). It was noted that the differences in standard deviation and CV between the EW and LW samples were greater for GP065 than GP258 (Tables 1a and 1b, respectively). Also, the mean MFA values for the LW samples were lower than those from the EW samples for both GP258 and GP065. Previous studies have found low MFA samples providing stronger calibration statistics (Jones *et al.* 2005, Schimleck *et al.* 2005) owing to the difficulties of measuring samples with high MFA. Schimleck *et al.* (2007) unexpectedly found that when both EW and LW sets employed seven factors, much weaker statistics resulted from the LW calibration, even with the lower MFA values. This was attributed to the possibility of the MFA measurement error remaining fairly constant over the measured MFA range.

The largest differences in mean MFA, as well as MFA range, standard deviation and CV were found between the corewood and outerwood (Tables 1a and 1b). The outerwood samples provided much greater MFA ranges, higher standard deviations and CVs than the corewood samples. Similarly, the large

differences in the calibration statistics were noted between the corewood and outerwood samples (Tables 2a and 2b). with better results obtained from the outerwood. It was found that the GP258 outerwood provided improved calibration results (R^2 = 0.72; SECV = 4.6°; RPD = 1.84) over the GP258 corewood (R^2 = 0.66; SECV = 2.6°; RPD = 1.65) despite the corewood calibration utilizing 15 factors. The GP065 corewood calibration was built using twice as many samples (994 samples) as the outerwood calibration (491 samples). Nevertheless, both calibrations were fitted using only 10 factors (Table 2b), and the same trends were observed as with the GP258 samples. Schimleck and coworkers also noted better correlations with greater MFA variation (Schimleck and Evans 2002, Schimleck *et al.* 2005). The same was found with calibrations for specific gravity, MOE and MOR (Schimleck *et al.* 2005), in which greater property variation was observed in the outerwood.

The calibrations obtained from the individual sample sets had the fewest number of samples, but compared with other studies, these small sample sets still had close to 240 samples for each calibration model. The individual corewood sample sets (EW4, EW5, LW4 and LW5) for GP258 employed between 11 and 13 factors, providing many of the poorest R^2 and RPD values (Tables 2a and 2b). The individual outerwood sample sets (EW19, EW20, LW19 and LW20) employed fewer factors, providing better R^2 values (Tables 2a and 2b); however, the resultant RPD values were only slightly better with higher SECV values. Similar behavior was observed with the GP065 sample sets. However, it is unclear as to the origin of the superior results obtained from the EW20 sample set. One point to note is that with these smaller individual sample sets, the differences between the SEC and SECV were relatively large as compared with the larger, combined sample sets mentioned earlier (Tables 2a and 2b). Nevertheless, these differences are still relatively small as compared with those found in the literature (Jones *et al.* 2006).

Prediction models

The performance of each calibration model was tested using the remaining unused quarter of each sample set, and assigned as the test sets. The predictions for these test sets were assessed using the coefficient of determination (R^2), SEP and RPD values. It can be seen that the calibrations performed reasonably well in predicting the MFA for both "All" GP258 and "All" GP065 test sets. The "All" GP258 calibration set consisted of 1897 samples and was evaluated using its corresponding test set of 629 samples (Table 2a). The prediction set provided slightly poorer results (10 factors; R^2 = 0.84; SEP = 4.4°; RPD = 2.47) to that from the calibration set. Kelley *et al.* (2004) reported poorer results (R^2 = 0.46 [R = 0.68]; RMSEP = 6.8°) from the small test set of 26 samples than those obtained from the calibration set (mentioned earlier in the Results section). In the case of the "All" GP065 samples, the prediction set provided almost identical results as with the calibration set. Similar trends were observed between the larger test and calibration sets from the GP065 samples (Table 2b). This was also observed in the EW and LW results for the GP258 samples (Table 2a). However, the individual GP258 test sets often provided better RPD values than their corresponding calibration sets. This was particularly true for individual "Core" sample sets (EW4, LW4, EW5 and LW5) and was evident with better "Core" test results (R^2 = 0.74; SEP = 2.4°; RPD = 1.96) than "Core" calibration results (R^2 = 0.66; SEP = 2.6°; RPD = 1.65), while the opposite was true with the "Outer" GP 258 samples. This may have been due, in part, to the difference in standard deviation between the corresponding test and calibration sets (Table 1a). Nevertheless, it was generally observed that these results still show the "All", "EW" and "LW" test sets as the best predictors of MFA with the highest RPD values.

In addition, these models were also tested using the corresponding test set from the other site. For example, the "All" GP258 calibration model (with 1897 samples) was first tested with the "All" GP258 test set (629 samples), followed by testing with the "All" GP065 test set (with 492 samples), and the results listed in Table 2b. The predictions for "All" GP065 (R^2 = 0.78; SEP = 4.9°; RPD = 2.00) did not improve upon those for "All" GP258 test set (R^2 = 0.84; SEP = 4.4°; RPD = 2.47). Testing was performed on all calibration models and in most cases, the corresponding test set from the opposite test site performed noticeably poorer than the test set from the same site. However, the magnitude of these differences in prediction may provide an indication of the value of applying the calibration models from one test site to predicting MFA from a different test site. The RPD values indicate some of these models are sufficient for screening purposes but the addition of more sites would provide more robust models possibly suitable for selection purposes. While sample preparation is a practical limitation with the high sample throughput utilized in genetics studies, this study was interested in analyzing individual growth rings. This cannot be achieved with NIR analysis of the radial-longitudinal face of a disk cut from the bole. The tangential face provided wood formed within the same growth period, as compared with the radial-longitudinal face, which is over a variable time period (Hein *et al.* 2010).

Regression coefficients

Regression coefficients are often used to relate how NIR data can be used to predict MFA (the orientation of the cellulose microfibrils in the secondary layers of the cell wall) and other wood properties. Fig. 3 shows the plot of regression coefficients for the GP258 "All" calibration, summarizing the relationship between wavelength and MFA, as approximated by the calibration model using 10 factors. This plot shows which NIR bands are important to the correlation between the NIR- and XRD-determined MFA values, providing information about the underlying relationships, allowing the estimation of MFA based on NIR spectra. There are several main bands influencing the correlations, including those at 1455, 1945, 2055, 2105, 2235, 2335 and 2360 nm. The bands around 2335 and 2352 nm have been assigned to cellulose, arising from a C-H stretch/C-H deformation and a CH_2 bending in the second overtone region, respectively (Shenk *et al.* 1992). Kelley *et al.* (2004) noted a peak found between 1890 nm and 2000 nm was related to OH combination bands, while Schimleck and Evans (2002) found large loadings associated with cellulose at 1470, 2082 and 2326 nm. Schimleck *et al.* (2007) noted a difference in loadings between their current study and an earlier one (Schimleck *et al.* 2005), both using samples of *Pinus taeda*, and attributed this to differences in the overall chemistry due to age and location of the samples. This present study collected samples from two progeny test sites in Ashley County, AR. The regression coefficient plots for the other calibrations (e.g., latewood) from both test sites were very similar to Fig. 3, only differing in the magnitude of the bands. Regression coefficients and loadings have previously been used to verify the inverse relationship between MFA and MOE (Kelley *et al.* 2004, Schimleck *et al.* 2005).

Conclusions

This study has shown that strong correlations can be obtained between NIR- and XRD-determined MFA using individual growth ring samples. The large data set allowed the comparisons of correlations between earlywood and latewood, corewood and outerwood, as well as individual growth rings. The larger data sets did appear to provide better models over the smaller individual data sets, with the predictive ability being greater. A greater variation in the number of sites would likely provide further improvement of model robustness. While allowing individual growth ring analysis, these correlations did not appear as strong as those obtained in other studies based on the radial-longitudinal face of wood strips, spread over several growth rings.

Acknowledgements

The authors would like to thank Karen Reed for the NIR spectra collection, and Robert Megraw for the MFA measurements.

References

Byram, T.D., J.H. Myszewski, D.P Gwaze and W.J. Lowe. 2005. Improving wood quality in the western gulf forest tree improvement program: the problem of multiple breeding objectives. Genet. Genomics. 1: 85–92.

Cave, I.D. and J.C.F. Walker. 1994. Stiffness of wood in fast-grown plantation softwoods: The influence of microfibril angle. For. Prod. J. 44: 43–48.

Clark, A., R.F. Daniels and L. Jordan. 2006. Juvenile/mature transition in loblolly pine as defined by annual ring specific gravity, proportion of latewood, and microfibril angle. Wood Fibre Sci. 38: 292–299.

Donaldson, L.A. 1991. The use of pit apertures as windows to measure microfibril angle in chemical pulp fibres. Wood Fibre Sci. 23: 290–295.

Donaldson, L. 2008. Microfibril angle: measurement, variation and relationships – a review in chemical pulp fibres. IAWA J. 29: 345–386.

El-Hosseiny, F. and D.H. Page. 1973. The measurement of fibril angle of wood fibres using polarized light. Wood Fibre Sci. 5: 208–214.

Evans, R. 1997. Rapid scanning of microfibril angle in increment cores by x-ray diffractometry. *In* B.G. Butterfield (ed.). Microfibril angle in wood. Proc. IAWA/IUFRO International Workshop on the Significance of Microfibril Angle to Wood Quality. pp. 116–139. University of Canterbury Press, Westport, New Zealand.

Evans, R. 1999. A variance approach to the x-ray diffractometric estimation of microfibril angle in wood. Appita J. 52: 283–289.

Evans, R. and J. Illic. 2001. Rapid prediction of wood stiffness from microfibril angle and density. For. Prod. J. 51: 53–57.

Gindl, W., A. Teischinger, M. Schwanninger and B. Hinterstoisser. 2001. The relationship between near infrared spectra of radial wood surfaces and wood mechanical properties. J. Near Infrared Spectrosc. 9: 255–261.

Groom, L., L. Mott and S. Shaler. 2002. Mechanical properties of individual southern pine fibres. Part II. Determination and variability of stress–strain curves with respect to tree height and juvenility. Wood Fibre Sci. 34: 14–27.

Hein, P.R.G., B. Clair, L. Brancheriau and G. Chaix. 2010. Predicting microfibril angle in Eucalyptus wood from different wood faces and surface qualities using near infrared spectra. J. Near Infrared Spectrosc. 18: 455–464.

Hoffmeyer, P. and J. Pedersen. 1995. Evaluation of density and strength of Norway spruce wood by near infrared reflectance spectroscopy. Holz Roh Werkst. 53: 165–170.

Jones, P.D., L.R. Schimleck, G.F. Peter, R.F. Daniels and A. Clark III. 2005. Nondestructive estimation of *Pinus taeda* L. wood properties for samples from a wide range of sites in Georgia. Can. J. For. Res. 35: 85–92.

Jones, P.D., L.R. Schimleck, G.F. Peter, R.F. Daniels and A. Clark III. 2006. Nondestructive estimation of wood chemical composition of sections of radial wood strips by diffuse reflectance near infrared spectroscopy. Wood. Sci Technol. 40: 709–720.

Kelley, S.S., T.G. Rials, R. Snell, L.H. Groom and A. Sluiter. 2004. Use of near infrared spectroscopy to measure the chemical and mechanical properties of solid wood. Wood Sci. Technol. 38: 257–276.

Martens, H. and T. Naes. 1989. Multivariate calibration. pp. 419. Wiley Press, Chichester, UK.

Megraw, R.A., G. Leaf and D. Bremer. 1998. Longitudinal shrinkage and microfibril angle in loblolly pine. *In* B.G. Butterfield (ed.). Microfibril angle in wood. Proc. IAWA/IUFRO International Workshop on the Significance of Microfibril Angle to Wood Quality. pp. 27–61. University of Canterbury Press, Westport, New Zealand.

Mott, L., L. Groom and S. Shaler. 2002. Mechanical properties of individual southern pine fibres. Part II. Comparison of earlywood and latewood fibres with respect to tree height and juvenility. Wood Fibre Sci. 34: 221–237.

Myszewski, J.H., F.E. Bridgwater, T.D. Byram, and R.A. Megraw. 2004. Genetic variation in the microfibril angle of loblolly pine from two test sites. South. J. Appl. For. 28: 196–204.

Shenk, J.S., J.J. Workman Jr. and M.O. Westerhaus. 1992. Application of NIR spectroscopy to agricultural products. *In* D.A. Burns and E.W. Ciurczak (eds.). Handbook of Near-Infrared Analysis. pp. 385–386. Marcel Dekker, New York.

Schimleck, L.R. and R. Evans. 2002. Estimation of microfibril angle of increment cores by near infrared spectroscopy. IAWA J. 23: 225–234.

Schimleck, L.R., R. Evans, P.D. Jones, R.F. Daniels, G.F. Peter and A. Clark III. 2005. Estimation of microfibril angle and stiffness by near infrared spectroscopy using samples sets having limited wood density variation. IAWA J. 26: 175–187.

Schimleck, L.R., E. Sussenbach, G. Leaf, P.D. Jones and C.L. Huang. 2007. Microfibril angle prediction of *Pinus taeda* wood samples based on tangential face NIR spectra. IAWA J. 28: 1–12.

Shupe, T.F., E.T. Choong, D.D. Stokke and M.D. Gibson. 1996. Variation in cell dimensions and fibril angle for two fertilized even-aged loblolly pine plantations. Wood Fibre Sci. 28: 268–275.

So C-L., B.K. Via, L.H. Groom, L.R. Schimleck, T.F. Shupe, S.S. Kelley and T.G. Rials. 2004. Near infrared spectroscopy in the forest products industry. For. Prod. J. 54: 6–16.

Via, B.K., C-L. So, L.H. Groom, T.F. Shupe, M. Stine and J. Wikaira. 2007. Within tree variation of lignin, extractives, and microfibril angle coupled with theoretical and near infrared modeling of microfibril angle. IAWA J. 28: 189–209.

Williams, P.C., D.C. Sobering. 1993. Comparison of commercial near infrared transmittance and reflectance instruments for the analysis of whole grains and seeds. J. Near Infrared Spectrosc. 1: 25–33.